Hemodynamic Aspect of Cerebral Watershed Infarction: Assessment of Perfusion Reserve Using Iodine-123-Iodoamphetamine SPECT

Hiroshi Moriwaki, Masayasu Matsumoto, Kazuo Hashikawa, Naohiko Oku, Mariko Ishida, Yujiro Seike, Yoshiyuki Watanabe, Hidetaka Hougaku, Nobuo Handa and Tsunehiko Nishimura

Division of Nuclear Medicine, First Department of Medicine, Department of Neurology and Department of Tracer Kinetics, Osaka University Medical School, Suita, Japan

The mechanism whereby watershed (WS) infarcts develop remains controversial, although a hemodynamic cause is usually assumed. The aim of this study was to investigate the relationship between the site of WS infarcts and the hemodynamic status of the cerebral circulation. **Methods:** From among 96 consecutive patients with angiographically confirmed unilateral major cerebral artery obstruction (occlusion or >70% stenosis), we investigated 29 patients with supratentorial WS infarcts on magnetic resonance imaging. The regional cerebral blood flow and perfusion reserve were quantified using the split-dose [^{123}I]iodoamphetamine SPECT method, coupled with intravenous injection of 1 g of acetazolamide. Seven patients had a cortical WS infarct between the superficial branches of the anterior and middle cerebral arteries (MCAs) or between the middle and posterior cerebral arteries (Group C), and 22 had a deep WS infarct between the superficial branches and deep penetrating arteries of the MCA (Group D). Moreover, the patients in Group D were classified into two subgroups, i.e., Type A (n = 12), with lesions lying in the centrum semiovale above the level of the lateral ventricles, and Type B (n = 10), with lesions lying in the corona radiata adjacent to the lateral ventricles. **Results:** Comparison of the Type of WS infarct with the clinical course of onset showed that sudden onset was more frequent in Group C than in Group D ($p < 0.05$). The perfusion reserve in the affected MCA territory in Group D (20.1% ± 15.6%) was significantly lower than that in Group C (43.8% ± 10.8%; $p < 0.01$) and that in 20 hemispheres (10 control subjects) without a major arterial lesion (54.7% ± 16.4%; $p < 0.01$). Among the Group D patients, the patients with Type A infarcts showed a significantly lower perfusion reserve compared with those with Type B infarcts ($p < 0.05$). **Conclusion:** Patients with deep WS infarcts, especially Type A infarcts, showed severe hemodynamic impairment, whereas patients with cortical WS infarcts showed preserved perfusion reserve which appeared to be secondary to the embolism. The mechanism of development of WS infarcts is multifactorial, and distinguishing among these WS infarcts and from other types of infarct is important, because different pathogenic mechanisms require different therapeutic strategies.

Key Words: watershed infarct; carotid artery diseases; perfusion reserve; SPECT; iodine-123-iodoamphetamine

J Nucl Med 1997; 38:1556–1562

Watershed (WS) infarcts are ischemic lesions that occur in the border zone between the territories of two major arteries. These border zones may be located superficially, between the interfaces of the areas supplied by the middle cerebral artery (MCA) and the anterior and posterior cerebral arteries or in the deep subcortical regions between medullary arteries, arising from the superficial pial plexus, and deep penetrating arteries, arising from the basal cerebral arteries (*1–3*). It is generally accepted that WS infarcts are caused by diminished perfusion of distal arteries, usually due to systemic hypotension (*4,5*) or internal carotid artery (ICA) occlusion (*1,2,5*). However, some WS infarcts seemed to be the result of vascular occlusion by thromboemboli, cholesterol emboli or tumor emboli (*5–8*). Both hemodynamics and microembolisms may cause WS infarcts, but the actual mechanism remains debatable (*5*).

Recently, using a PET system, several authors have examined the hemodynamic status in ICA occlusive disease to test the hypothesis that the cortical WS area is selectively vulnerable, but, again, their results remain controversial (*9–11*). On the other hand, Weiller et al. (*12*) and Yamauchi et al. (*13*) examined the relationship between the presence of deep WS infarcts and the hemodynamic status of the cerebral cortex. However, to our knowledge, few reports have detailed the relationship between the occurrence of WS infarcts, including both cortical and deep WS infarcts, and the hemodynamic status of the cerebral circulation.

By means of a widely available [^{123}I]iodoamphetamine ([^{123}I]IMP) and SPECT system, we have developed the "split-dose [^{123}I]IMP SPECT method" (*14*), which enables quantitative measurement of the regional cerebral blood flow (rCBF) under two different conditions within a short time. Using this method, coupled with acetazolamide challenge, we were able to evaluate the resting rCBF and regional perfusion reserve quantitatively. In this study, we investigated the relationship between the site of WS infarcts and the hemodynamic status in occlusive disease of the carotid system to examine whether the WS infarct is, in fact, a sign of hemodynamic compromise.

MATERIALS AND METHODS

Patients

From among 96 consecutive patients who had a unilateral occlusion or severe stenosis (>70% in diameter) in the ICA or in the main trunk of the MCA, we selected 29 patients [25 men and 4 women, aged 62.3 ± 9.1 yr (mean ± s.d.)] with evidence of supratentorial WS infarcts documented by magnetic resonance imaging (MRI). These patients were inpatients or outpatients at the First Department of Internal Medicine, Osaka University Medical School Hospital. Patients were excluded if they had a cerebral infarction larger than 3 cm in the long axis on MRI in an area other than the WS area. Those who had a cardioembolic risk factor, such as atrial fibrillation, valvular heart disease or myocardial infarction, were also excluded (*15*). Brain MRI, cerebral angiography and SPECT study with acetazolamide challenge were performed in all subjects.

The vascular lesions were present in the ICA in 20 patients and in the main trunk of the MCA in nine. Silent cerebral infarction was

Received Jul. 25, 1996; revision accepted Dec. 19, 1996.

For correspondence or reprints contact: Hiroshi Moriwaki, MD, First Department of Internal Medicine, Osaka University Medical School, 2-2 Yamadaoka, Suita 565, Japan.

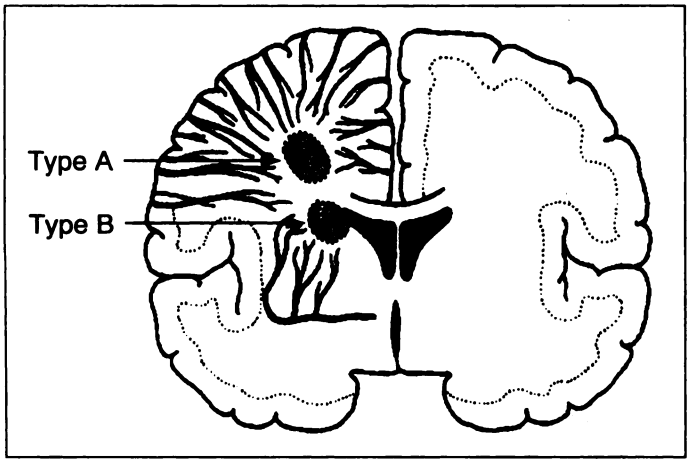

FIGURE 1. Schematic diagram showing the border zone between the superficial branches and the deep perforators of the MCA, with shaded areas being susceptible to infarction. Type A indicates a lesion lying in the centrum semiovale, above the level of the lateral ventricles. Type B indicates a lesion lying in the corona radiata, adjacent to the lateral ventricles.

present in six patients, transient ischemic attacks was present in three and completed stroke was present in 20. Of 23 symptomatic patients, the clinical course of onset was sudden in 13, and in 10, subacute, manifesting neurological defects evolved over more than several hours.

We determined the WS area according to the templates of Bogousslavsky and Regli (*1*) and the atlas of Damasio (*16*). Two types of WS infarcts were identified, one being cortical WS infarcts, involving the regions between the superficial territories of the MCA and the anterior cerebral artery and/or between the MCA and the posterior cerebral artery, and the other being deep WS infarcts between the superficial branches and deep penetrating arteries of the MCA. A cortical WS infarct was seen in 10 patients, and a deep WS infarct was seen in 22; three patients had infarcts in both cortical and deep WS areas. We classified the patients into two groups: seven patients with a WS infarct only in the cortical WS area (Group C) and 22 patients with a deep WS infarct (Group D). Moreover, the patients in Group D were classified into two subgroups according to Zülch (*3*) (Fig. 1), i.e., Type A (n = 12), with lesions lying in the centrum semiovale above the level of the lateral ventricles, and Type B (n = 10), with lesions lying in the corona radiata adjacent to the lateral ventricles. The clinical and neuroradiological characteristics of each patient are summarized in Tables 1 and 2.

As presented in Table 3, we evaluated another group of eight consecutive patients who had cortical WS infarcts depicted by MRI, with stenotic lesions less than 70% in diameter in the ICA or in the main trunk of the MCA (Group CN, aged 65.9 ± 9.0 yr). These patients were selected to compare with Group C. Patients with a potential cardiac source of emboli were included in Group CN.

Ten age-matched patients with a complaint of the nonfocal neurological symptom of dizziness or headache underwent SPECT studies to determine the normal values (Group NS, aged 64.8 ± 6.8 yr). In these cases, no ischemic lesions were detected by MRI and no stenotic lesions in the major cerebral arteries were detected by magnetic resonance angiography (MRA).

The study protocol was in accordance with the standard ethical guidelines of Osaka University Medical School, and informed consent was obtained from all subjects.

Brain MRI Scan

MRI was performed before the SPECT study with a 1.5-T unit in the orbito-meatal plane with 10-mm-thick sections. Infarction was defined as a focal area with prolonged T1 and T2 relaxation times larger than 5 mm in diameter (*17*). The interval between MRI

TABLE 1
Characteristics of Patients with Deep WS Infarcts (Group D)

Patient no.	Age (yr)	Sex	Neurological deficit	Type of ischemia	Type of onset	Angiographic findings	MRI lesions
Type A							
1	56	M	L hemiparesis, dysarthria	CS	Subacute	R ICA O	R CO, R corona radiata
2	53	F	R hemiparesis, aphasia	CS	Subacute	L ICA S (90%)	L CO, L corona radiata
3	42	M	R hemiparesis	CS	Sudden	L MCA O	L CO, L temporal
4	67	M	R VD	CS	Subacute	R ICA O	R CO
5	53	M	None	Asymptomatic	(−)	L ICA O	L CO, L corona radiata
6	68	M	None	Asymptomatic	(−)	L ICA O	L CO
7	71	M	R hemiparesis, L VD	CS	Subacute	L ICA O	L CO
8	65	M	R hemiparesis, aphasia	CS	Subacute	L ICA S (99%), R ICA S (50%)	L CO, L temporal
9	44	M	R hemiparesis	TIA	Sudden	L MCA O	L CO, L BG
10	68	M	Dysarthria	TIA	Subacute	L MCA O	L CO, L PWS
11	66	M	L hemiparesis	CS	Subacute	R ICA O	R CO, R PWS
12	73	M	L hemiparesis	CS	Subacute	R ICA O, L ICA S (50%)	R CO, R AWS
Type B							
13	69	F	None	Asymptomatic	(−)	R ICA S (90%)	R corona radiata, R frontal
14	58	M	L hemiparesis	CS	Sudden	R MCA O	R corona radiata
15	69	F	None	Asymptomatic	(−)	R ICA S (70%), L ICA S (50%)	R corona radiata
16	68	M	None	Asymptomatic	(−)	R ICA S (70%) + ulcer	R corona radiata, R BG
17	59	M	None	Asymptomatic	(−)	R ICA O	R corona radiata, R frontal
18	71	M	Dysarthria	TIA	Sudden	R ICA S (70%)	R corona radiata, R BG, L BG
19	52	M	R hemiparesis, dysarthria	CS	Subacute	L MCA S (90%), R ICA S (50%)	L corona radiata
20	58	M	L hemiparesis	CS	Sudden	R MCA O	R corona radiata, R temporal
21	73	F	Syncope, L hemiparesis	CS	Sudden	R ICA S (70%) + ulcer	R corona radiata
22	71	M	R hemiparesis	CS	Sudden	L ICA O	L corona radiata

L = left; R = right; VD = visual disturbance; CS = completed stroke; TIA = transient ischemic attack; O = occlusion; S = stenosis; ulcer = ulceration; CO = centrum semiovale; BG = basal ganglia; PWS = posterior WS; AWS = anterior WS.

TABLE 2
Characteristics of Patients with Cortical WS Infarcts with Ipsilateral Stenosis (Group C)

Patient no.	Age (yr)	Sex	Neurological deficit	Type of ischemia	Type of onset	Angiographic findings	MRI lesions
23	59	M	R hemiparesis	CS	Sudden	L MCA O	L PWS
24	70	M	L hemiparesis	CS	Sudden	R ICA S (90%)	R PWS
25	77	M	L hemiparesis	CS	Sudden	R ICA O, L ICA S (50%)	R PWS, R temporal
26	50	M	L numbness, dysarthria	CS	Subacute	R MCA S (90%)	R PWS
27	49	M	L hemiparesis	CS	Sudden	R MCA S (90%)	R PWS, R BG
28	64	M	R hemiparesis	CS	Sudden	L ICA S (80%), R ICA S (40%)	L AWS
29	63	M	R hemiparesis	CS	Sudden	L ICA S (70%) + ulcer	L PWS, L parietal

R = right; L = left; CS = completed stroke; O = occlusion; S = stenosis; ulcer = ulceration; PWS = posterior WS; AWS = anterior WS; BG = basal ganglia.

and SPECT study was within 7 days (mean, 2.8 ± 1.3 days). Two radiologists, who were blinded to all clinical information, independently reviewed the MRIs.

Brain SPECT Study

The SPECT study was performed at least 4 wk after the patient's last clinical episode, when the neurological conditions had become stable. The details of our SPECT study with acetazolamide challenge have been reported elsewhere (*14*). In brief, we used a high-performance, four-head rotating gamma camera equipped with low-energy, general-purpose, parallel-hole collimators with a 13.0-mm FWHM (*18*). Data were acquired in a continuous rotating mode in reciprocal directions at 20 sec/revolution for 58 min, 14 frames with 8 revolutions followed by 2 frames with 32 revolutions, from 64 directions in a 64 × 64 matrix. During dynamic SPECT, 111 MBq of [^{123}I]IMP was injected intravenously at the beginning of imaging and again at the start of the 10th frame of acquisition, with continuous arterial blood sampling for 332 sec after each injection. One gram of acetazolamide was slowly injected intravenously for 1 min, at the start of the fourth frame of acquisition. The rCBF values were quantified by the microsphere method using the octanol extraction activities of arterial samplings (*19*). The resting CBF image was reconstructed from the summation of the second-to-ninth-frame data. The acetazolamide challenge CBF image was reconstructed from the summation of the 11th-to-16th-frame data, with subtraction of the remaining brain activity due to the first [^{123}I]IMP injection. The 8-mm-slice transaxial images were reconstructed using a Butterworth filter as the prefilter and a Ramachandran filter as the reconstruction filter.

Region of interest (ROI) analysis in this study is illustrated in Figure 2. On the thalamo-basal transaxial slice in the resting CBF image, the 50% iso-accumulation line of the maximum value was outlined to trace the contour of the cerebrum. The outlined cerebral area was automatically divided into four equally sized longitudinal ROIs, and bilateral outer ROIs corresponded to bilateral MCA territories (*20*). In Groups D, C and CN, the affected MCA territory was evaluated, and in Group NS, bilateral MCA territories were evaluated. If an infarct was included within this standard ROI, the size of ROI was reduced to avoid the infarct. All ROIs generated in the resting image were transferred to the acetazolamide challenge image. The percent increase of rCBF induced by acetazolamide challenge (%INC) was estimated as the vascular perfusion reserve as follows (*14*): %INC = [CBF(ACZ) − CBF(rest)]/CBF(rest) × 100, where CBF(ACZ) and CBF(rest) represent the CBF in the acetazolamide-challenge state and in the resting state, respectively.

TABLE 3
Characteristics of Patients with Cortical WS Infarcts Without Stenosis (Group CN)

Patient no.	Age (yr)	Sex	Neurological deficit	Type of ischemia	Type of onset	Angiographic findings	Cardiac disease	MRI lesions
30	46	M	R hemiparesis	CS	Sudden	(−)* R temporal	Af	L AWS, L PWS
31	64	M	Gait disturbance	CS	Sudden	(−)	Af	R PWS, L thalamus
32	65	M	R hemiparesis	CS	Sudden	(−)	Af	L PWS
33	62	M	L hemiparesis	CS	Sudden	R ICA S (30%)	OMI, hypokinetic LV segment	R PWS
34	70	M	R homonymous hemianopsia dyscalculia	CS	Sudden	L ICA S (30%) + ulcer	(−)	L PWS
35	77	M	R hemiparesis	CS	Sudden	(−)*	OMI, akinetic LV segment	L PWS
36	75	M	R homonymous hemianopsia	CS	Sudden	L ICA S (30%) R ICA S (50%)	OMI, asynergy (−)	L PWS, L thalamus
37	68	M	L amaurosis fugax	TIA	Sudden	L ICA S (40%) + ulcer	(−)	L PWS

*MRA.

R = right; L = left; CS = completed stroke; TIA = transient ischemic attack; S = stenosis; ulcer = ulceration; Af = atrial fibrillation; OMI = old myocardial infarction; LV = left ventricle; AWS = anterior WS; PWS = posterior WS.

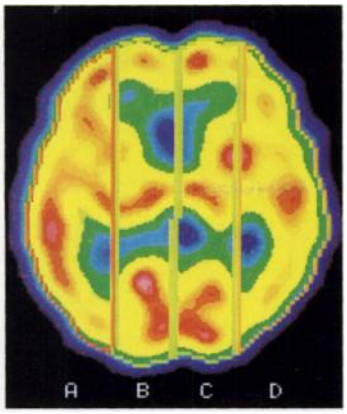

FIGURE 2. ROI used in the SPECT analysis. On thalamo-basal transaxial slice, the outlined cerebral area was automatically divided into four equally sized longitudinal ROIs (A–D), and bilateral outer ROIs correspond to bilateral MCA territories (A and D).

Angiography

Conventional angiography or digital subtraction intra-arterial angiography (DSA) was performed in 96 patients, including all patients in Groups C and D (35 patients by conventional angiography and 61 patients by DSA) and 6 patients in Group CN (2 patients by conventional angiography and 4 patients by DSA). The maximum percent stenosis and the presence of ulceration, which may cause artery-to-artery embolism (*15,21*), were evaluated according to the recommendations of the North American Symptomatic Carotid Endarterectomy Trial (NASCET) (*22*). In two patients in Group CN and all patients in Group NS, invasive angiography was not performed. Their carotid and intracranial lesions were evaluated using noninvasive three-dimensional time-of-flight MRA (*23*).

Statistical Analysis

Data were analyzed by the chi-square test and Student's t-test. Parametric comparisons of measured data obtained in more than three groups were performed by ANOVA. Scheffe's multiple comparison test was used to examine the relationship between variables. A difference of $p < 0.05$ was considered significant. The results were expressed as the mean ± s.d.

RESULTS

There were no serious adverse effects of acetazolamide administration, although three patients complained of minor side effects, including facial numbness and dizziness.

Comparison of the type of WS infarct with the clinical course of onset showed that sudden onset was more frequent in Group C (6/7; 86%) than in Group D (7/22; 32%) ($p < 0.05$) (Tables 1 and 2). Among Group D patients, subacute onset was more frequent in the patients with Type A (8/12; 67%) than in those with Type B (1/10; 10%) ($p < 0.05$). All patients with infarcts in both cortical and deep WS areas showed subacute onset (Patients 10–12 in Table 1).

TABLE 4
rCBF and Perfusion Reserve of the Affected MCA Territories

Group	n	Mean rCBF (ml/min/100 gr) Rest	Acetazolamide	%INC
D	22	38.3 ± 5.5*	46.3 ± 10.4*†	20.1 ± 15.6*†‡
	12 (type A)	37.0 ± 5.5	42.5 ± 10.7	13.6 ± 15.2§
	10 (type B)	39.8 ± 5.4	50.9 ± 8.4	27.9 ± 12.6
C	7	40.7 ± 4.8	58.5 ± 8.0	43.8 ± 10.8
CN	8	41.0 ± 5.9	62.4 ± 7.5	52.8 ± 12.8
NS	20	44.8 ± 6.3	69.1 ± 10.5	54.7 ± 16.4

D = deep WS infarct; C = cortical WS infarct; CN = cortical WS infarct without a major arterial lesion; NS = control group; Type A = the lesion lies in the centrum semiovale, above the level of the lateral ventricles; Type B = the lesion lies in the corona radiata, adjacent to the lateral ventricle. Values are expressed as mean ± s.d.

*$p < 0.01$ vs. Group NS.

†$p < 0.01$ vs. Group CN.

‡$p < 0.01$ vs. Group C by Scheffe's multiple comparison after ANOVA.

§$p < 0.05$ vs. Type B by Student's unpaired t-test.

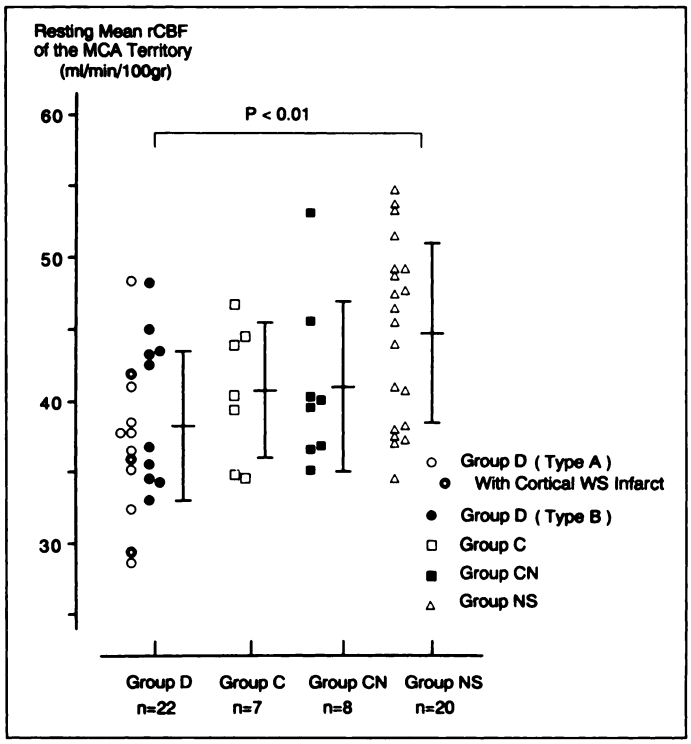

FIGURE 3. Plot showing the resting mean rCBF values of the affected MCA territory in each group of subjects. The resting rCBF value in Group D was significantly lower than that in Group NS. There were no significant differences between Groups C or CN and D and between Groups C or CN and NS. Groups D, C, CN and NS represent the deep WS infarct, cortical WS infarct, cortical WS infarct without a major arterial lesion and control group, respectively.

As shown in Table 3, all eight patients in Group CN experienced sudden onset. Among them, cardiac disease, which might have caused cardiogenic embolism, was found in five patients, and carotid ulceration, which might have caused artery-to-artery embolism, was found in two patients without cardiac disease.

Table 4 summarizes the mean rCBF values in the resting and acetazolamide-challenge states and the %INCs in the affected MCA territories in each group. As shown in Figure 3, the resting rCBF value in Group D was significantly lower than that in Group NS (38.3 ± 5.5 ml/min/100 g versus 44.8 ± 6.3 ml/min/100 g; $p < 0.01$). However, the distributions of rCBF values overlapped widely among the subjects in each group, and there were no significant differences among the other combination of Groups. Figure 4 shows the %INC of each group of subjects. The %INC in Group D (20.1% ± 15.6%) was significantly lower than in Groups C, CN and NS (43.8% ± 10.8%, 52.8% ± 12.8% and 54.7% ± 16.4%, respectively). There were no significant differences among Groups C, CN and NS in terms of the %INC. Among the Group D patients, patients with Type A infarcts showed a significantly lower %INC compared with patients with Type B infarcts (13.6% ± 15.2% versus 27.9% ± 12.6%; $p < 0.05$). Figure 5 demonstrates typical MRI and SPECT images in a patient of Group D (Patient 1). MRI shows deep WS infarcts in the centrum semiovale and corona radiata of the right side, with no involvement in the cerebral cortex. SPECT images demonstrate low

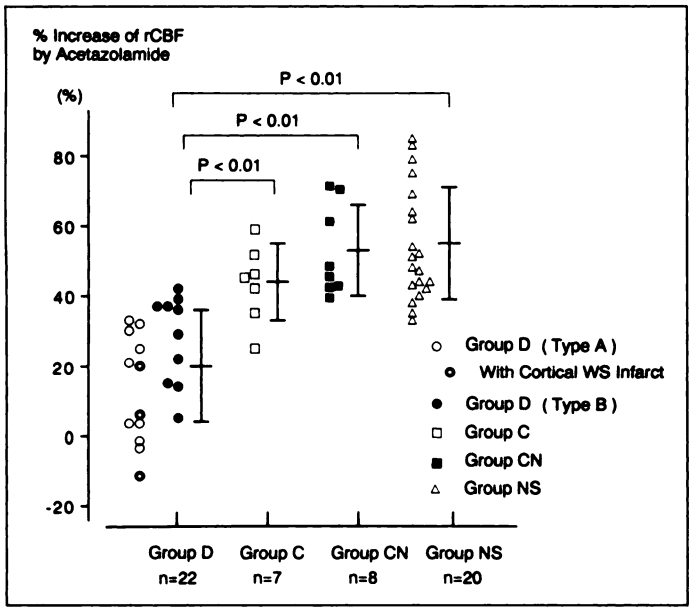

FIGURE 4. Plot showing the %INC of rCBF values of the affected MCA territory induced by acetazolamide in each group of subjects. Significantly decreased %INC in Group D was observed and compared with the other three groups: Groups C, CN and NS. Groups D, C, CN and NS represent the deep WS infarct, cortical WS infarct, cortical WS infarct without a major arterial lesion and control group, respectively.

perfusion and decreased acetazolamide reactivity in the right MCA territory (%INC = 4.7%). Figure 6 shows MRI and SPECT images in a patient of Group C (Patient 24). MRI shows posterior WS infarction. SPECT images reveals preserved CBF and acetazolamide reactivity except for the infarcted area (%INC = 46.4%).

All patients with infarcts in both cortical and deep WS areas (n = 3) had Type A infarcts in the deep WS area. The resting rCBF of these patients (35.8 ± 6.3 ml/min/100 g) was significantly lower than that of Group NS ($p < 0.05$), but not significantly different from those of Groups C and CN. Their %INC (5.3% ± 15.6%) was significantly lower than that in Group C ($p < 0.05$), but it was not significantly different from that of 19 patients with deep WS infarcts alone.

DISCUSSION

In this study, WS infarcts were found in 30.2% (29/96) of patients examined, with cortical WS infarcts in 10.4% (10/96) and deep WS infarcts in 22.9% (22/96). The incidence of WS infarcts was similar to the previously reported incidence (7–40%) of WS infarcts in patients with ICA occlusion or severe stenosis (*2,24,25*). Bogousslavsky et al. (*1*) reported on 51 patients with WS infarcts from a computed tomography study and found that 80% of WS infarcts were cortical WS infarcts, whereas only 20% were deep WS infarcts. The high prevalence of deep WS infarcts in our study is presumably because we diagnosed WS infarcts by MRI, the most sensitive method for evaluating organic changes in the brain, including the white matter. Of course, the possibility of false identification of large Virchow-Robin spaces as deep WS infarcts cannot be completely ruled out (*26*).

In this study, patients with deep WS infarcts, both with and without a combination of cortical WS infarcts, showed reduced perfusion reserve compared with the controls. The clinical course of onset of them was sudden in seven cases and subacute in nine cases. On the other hand, patients with cortical WS infarcts alone, both with and without major arterial disease, showed preserved perfusion reserve. In most of these patients,

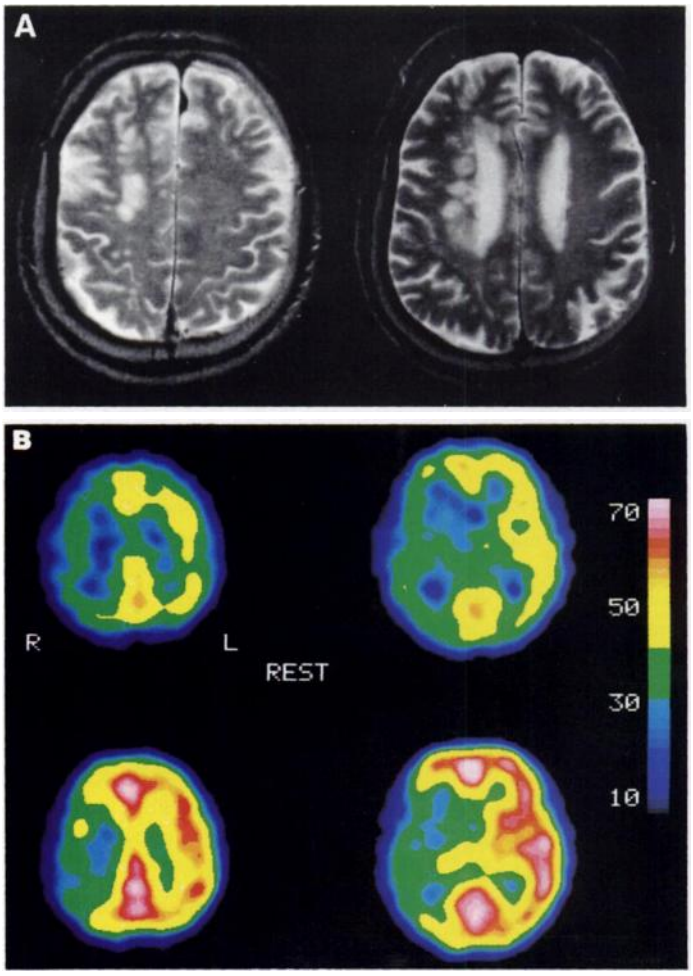

FIGURE 5. Representative MRI and SPECT images in a patient of deep WS infarct (Patient 1, Type A). (A) MRI shows deep WS infarcts in the centrum semiovale and corona radiata of the right side, while no involvement in the cerebral cortex. (B) SPECT images demonstrate low perfusion and decreased acetazolamide reactivity in the right MCA territory (%INC = 4.7%).

the onset had been sudden. In addition, although the actual mechanism was not clear, seven of the eight patients in group CN had an embolic source that might have caused cardiogenic embolism or artery-to-artery embolism (*15,21*). These results support the embolic theory of cortical WS infarcts.

Classically, it has generally been thought that most cortical WS infarcts arise by a hemodynamic mechanism (*1,2,4*). These typically occur when a patient with severe carotid artery stenosis experiences a decrease in the systemic blood pressure (*1,27*) or when a patient acutely develops on ICA occlusion (*25*). However, some authors (*6,7,28,29*) have suggested that embolization may play a major role in the genesis of cortical WS infarcts. Torvik et al. (*6*) examined 18 autopsy cases with cortical WS infarcts and postulated that WS infarcts can be produced by showers of microemboli, which tend to lodge in the terminal vascular fields. Masuda et al. (*28*) recently studied 15 autopsy cases with cerebral atheromatous embolism and reported that 9 of them had infarcts in the WS area and only 6 cases had territorial infarcts. The mechanism behind the preferential distribution of emboli to cortical WS regions may involve the arterial branch angle (*6*) and arterial branch diameter (*7,29*). Pollanen et al. (*29*) reported, based on experimental studies, that emboli in the 150–210-μm size range selectively propagated in the cortical WS area. Our findings that hemodynamic mechanisms were not consistently involved provide further support for the embolic theory of cortical WS infarcts.

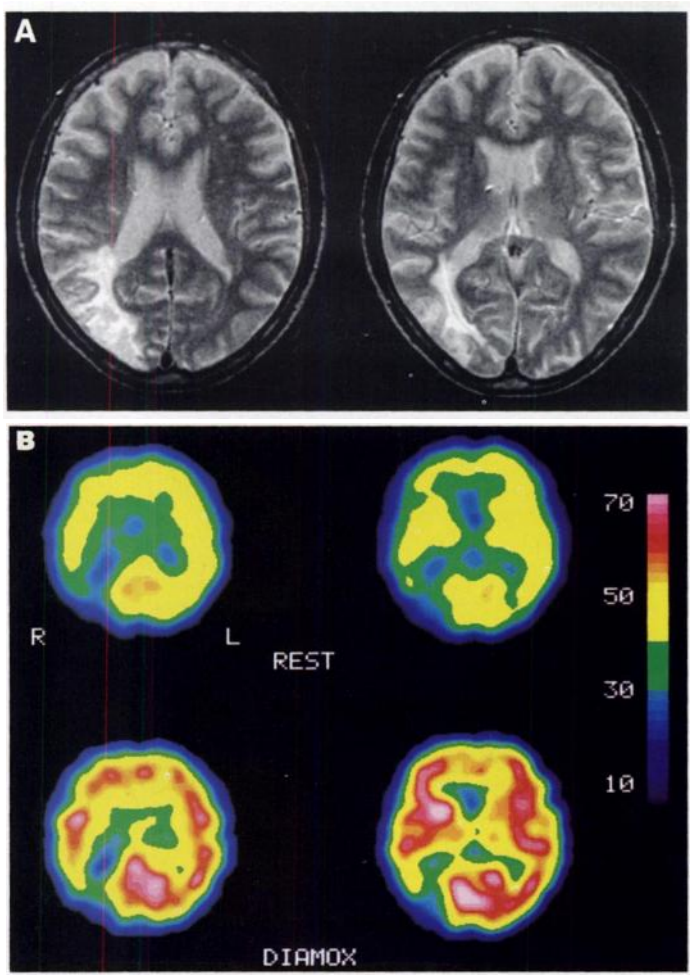

FIGURE 6. Representative MRI and SPECT images in a patient of cortical WS infarct (Patient 24). (A) MRI shows cortical WS infarct between the MCA and posterior cerebral artery of the right side. (B) SPECT images reveal preserved resting CBF and acetazolamide reactivity, except for the infarcted area (%INC = 46.4%).

Of course, in individual cases, cortical WS infarcts might be caused by other mechanisms, such as a hemodynamic mechanism and territorial thrombosis (*5*).

On the other hand, patients with deep WS infarcts showed a decreased perfusion reserve. This is in accordance with the observations of Weiller et al. (*12*) and Hupperts et al. (*30*), who suggested that deep WS infarcts indicate hemodynamic compromise. However, the wide range of %INC values in our Group D patients suggests partial participation of other mechanisms, such as embolism and thrombosis. Additionally, we should consider the potential role of embolism superimposed on perfusion impairment. Deep WS infarcts are commonly small on MRI; however, the majority of them represent only a small visible trace of profound decreased perfusion reserve. Because compromised perfusion reserve is associated with an increased risk of stroke in the near future (*31*), deep WS infarcts visualized on MRI should become a common indication for further investigation of the cerebral circulation.

We subclassified the deep WS infarcts into two subgroups according to Zülch (*3*). We found that Type A patients seemed to show the influence of a hemodynamic factor more strongly compared with Type B patients. Yamauchi et al. (*13*) examined ICA occlusive disease using PET and reported that patients with a high-intensity area on T2-weighted MRI in the middle centrum semiovale, located in the same site as that in our Type A patients, showed severe hemodynamic compromise. Although most of the previous studies of deep WS infarcts did not distinguish between these two subtypes (*12,30,32*), our results suggest the possibility of a multifactorial mechanism and the necessity to classify deep WS infarcts into the Type A and B subgroups.

The %INC of patients with infarcts in both cortical and deep WS areas was similar to that of patients with a deep WS infarct alone but different from that of patients with a cortical WS infarct alone. Hemodynamic mechanisms seem to play a major role in the genesis of such types of infarcts. In the case of cortical WS infarcts, it is important to determine the presence or absence of coexistent deep WS infarcts to examine the pathogenic mechanism.

In this study, we evaluated the rCBF and perfusion reserve using the split-dose [^{123}I]IMP SPECT method (*14*). PET is a powerful tool for assessing cerebrovascular disease, which provides quantitative information about the rCBF, metabolism and other physiological parameters, such as the oxygen extraction fraction (*9,33*). However, a cyclotron-based PET system involves high cost and manpower for daily clinical use. On the other hand, our split-dose [^{123}I]IMP SPECT method with acetazolamide challenge, which allows for the quantification of the rCBF values and perfusion reserve within a short time, is applicable for clinical use (*14*). The mean response to acetazolamide in Group NS was 54.7%, which is in agreement with most previous studies using PET or using ^{133}Xe inhalation with SPECT (*33,34*). There was a significant difference between Group D and Group NS in terms of their resting rCBF values, although the distributions of these values widely overlapped among the groups (Fig. 3). For the investigation of pathophysiology of cerebrovascular disease, absolute quantification of the rCBF values is important, especially to select candidate patients for revascularization surgery and to evaluate bilateral carotid artery disease (*33,35*). However, the resting rCBF values alone do not fully predict the cerebral hemodynamics in individual cases, and the perfusion reserve (%INC) could be considered a more stable and better parameter (Fig. 4).

In this study, we determined the MCA ROIs automatically as a reproducible procedure, including both cortical and subcortical area. In case of Group D patients, evaluation of the actual rCBF in the subcortical white matter might be preferable, but, because of the characteristics of [^{123}I]IMP distribution, which are decreasing from gray to white matter and partial volume effects, its evaluation by [^{123}I]IMP SPECT is difficult (*19,36,37*). On the other hand, small subcortical lesions, such as deep WS infarcts, sometimes cause a reduction of cortical CBF, what is called "intrahemispheric diaschisis" (*35,38*). However, Takano et al. (*39*) reported using ^{133}Xe intracarotid injection and carbon dioxide inhalation method that the vascular reactivity of the cortical area with intrahemispheric diaschisis is preserved. Therefore, the reduction of %INC in Group D patients is due to hemodynamic compromise and is not merely a result of intrahemispheric diaschisis.

We determined the WS area as accurately as possible using MRI and an atlas (*1,16*). However, the individual variability of cerebral arterial territories and, consequently, of the location of the WS area is reported to be much greater than was previously recognized (*40*). Therefore, there is a possibility that we may mistake some territorial infarcts as cortical WS infarcts. On the other hand, we must distinguish deep WS infarcts from other subcortical infarcts depicted on MRI. Lacunae are smaller (<1.5 cm in diameter) and located in the basal ganglia and internal capsule, at a lower plane (*41*). There should be no confusion with striatocapsular infarction, which often produces

a comma-shaped lesion on MRI and occurs at a lower plane, with involvement of the internal capsule and striatum (*42*).

CONCLUSION

This study indicated that patients with deep WS infarcts, especially Type A infarcts, showed severe hemodynamic impairment, whereas patients with cortical WS infarcts showed preserved perfusion reserve, which appeared to be secondary to the embolism. Thus, deep WS infarcts on MRI should subsequently become a common indication for further investigation of the cerebral circulation. The mechanism of development of WS infarcts was multifactorial, and distinguishing these WS infarcts from other types of infarcts, such as lacunar and other subcortical infarcts, is important, because different pathogenic mechanisms require different therapeutic strategies.

ACKNOWLEDGMENTS

This work was supported by a grant for cardiovascular diseases from the Japanese Ministry of Health and Welfare and, in part, by the Smoking Research Foundation. We thank M. Shimomura, R. Manabe and N. Hinokami for their invaluable secretarial assistance.

REFERENCES

1. Bogousslavsky J, Regli F. Unilateral cerebral watershed infarcts. *Neurology* 1986;36: 373–377.
2. Wodarz R. Watershed infarctions and computed tomography. A topographical study in cases with stenosis or occlusion of the carotid artery. *Neuroradiology* 1980;19:245–248.
3. Zülch KJ. On the development and localization of brain infarction. *Zentralbl Neurochir* 1961;21:158–178.
4. Adams JH, Brierley JB, Connor RCR, Treip CS. The effects of systemic hypotension upon the human brain: clinical and neuropathological observations in 11 cases. *Brain* 1966;89:235–268.
5. Torvik A. The pathogenesis of watershed infarcts in the brain. *Stroke* 1984;15:221–223.
6. Torvik A, Skullerud K. Watershed infarcts in the brain caused by microemboli. *Clin Neuropathol* 1982;1:99–105.
7. Pollanen MS, Deck JHN. Directed embolization is an alternate cause of cerebral watershed infarction. *Arch Pathol Lab Med* 1989;113:1139–1141.
8. Beal MF, Williams RS, Richardson EP Jr, Fisher CM. Cholesterol embolism as a cause of transient ischemic attacks and cerebral infarction. *Neurology* 1981;31:860–865.
9. Yamauchi H, Fukuyama H, Kimura J, Konishi J, Kameyama M. Hemodynamics in internal carotid artery occlusion examined by positron emission tomography. *Stroke* 1990;21:1400–1406.
10. Leblanc R, Yamamoto YL, Tyler JL, Hakim A. Hemodynamic and metabolic effects of extracranial carotid disease. *Can J Neurol Sci* 1989;16:51–57.
11. Carpenter DA, Grubb RL Jr, Powers WJ. Borderzone hemodynamics in cerebrovascular disease. *Neurology* 1990;40:1587–1592.
12. Weiller C, Ringelstein EB, Reiche W, Buell U. Clinical and hemodynamic aspects of low-flow infarcts. *Stroke* 1991;22:1117–1123.
13. Yamauchi H, Fukuyama H, Yamaguchi S, Miyoshi T, Kimura J, Konishi J. High-intensity area in the deep white matter indicating hemodynamic compromise in internal carotid artery occlusive disorders. *Arch Neurol* 1991;48:1067–1071.
14. Hashikawa K, Matsumoto M, Moriwaki H, et al. Split dose iodine-123-IMP SPECT: sequential quantitative regional cerebral blood flow change with pharmacological intervention. *J Nucl Med* 1994;35:1226–1233.
15. Whisnant JP, Basford JR, Bernstein EF, et al. Classification of cerebrovascular diseases III. *Stroke* 1990;21:637–676.
16. Damasio H. A computed tomographic guide to the identification of cerebral vascular territories. *Arch Neurol* 1983;40:138–142.
17. Hougaku H, Matsumoto M, Kitagawa K, et al. Silent cerebral infarction as a form of hypertensive target organ damage in the brain. *Hypertension* 1992;20:816–820.
18. Kimura K, Hashikawa K, Etani H, et al. A new apparatus for brain imaging: four-head rotating gamma camera single-photon emission computed tomograph. *J Nucl Med* 1990;31:603–609.
19. Kuhl DE, Barrio JR, Huang SC, et al. Quantitative local cerebral blood flow by N-isopropyl-p-[^{123}I]iodoamphetamine tomography. *J Nucl Med* 1982;23:196–203.
20. Oku N, Matsumoto M, Hashikawa K, et al. Carbon dioxide reactivity by consecutive technetium-99m-HMPAO SPECT in patients with a chronically obstructed major cerebral artery. *J Nucl Med* 1994;35:32–40.
21. Moriwaki H, Matsumoto M, Handa N, et al. Functional and anatomic evaluation of carotid atherothrombosis: a combined study of indium 111 platelet scintigraphy and B-mode ultrasonography. *Arterioscler Thromb Vasc Biol* 1995;15:2234–2240.
22. North American Symptomatic Carotid Endarterectomy Trial Steering Committee. North American Symptomatic Carotid Endarterectomy Trial: methods, patient characteristics and progress. *Stroke* 1991;22:711–720.
23. Mandai K, Sueyoshi K, Fukunaga R, et al. Evaluation of cerebral vasoreactivity by three-dimensional time-of-flight magnetic resonance angiography. *Stroke* 1994;25: 1807–1811.
24. Ringelstein EB, Zeumer H, Angelou D. The pathogenesis of strokes from internal carotid artery occlusion. Diagnostic and therapeutical implications. *Stroke* 1983;14: 867–875.
25. Bogousslavsky J, Regli F. Borderzone infarctions distal to internal carotid artery occlusion: prognostic implications. *Ann Neurol* 1986;20:346–350.
26. Heier LA, Bauer CJ, Schwartz L, Zimmerman RD, Morgello S, Deck MDF. Large Virchow-Robin spaces: MR-clinical correlation. *Am J Neuroradiol* 1989;10:929–936.
27. Howard R, Trend P, Ross Russell RW. Clinical features of ischemia in cerebral arterial border zones after periods of reduced cerebral blood flow. *Arch Neurol* 1987;44:934–940.
28. Masuda J, Yutani C, Ogata J, Kuriyama Y, Yamaguchi T. Atheromatous embolism in the brain: a clinicopathologic analysis of 15 autopsy cases. *Neurology* 1994;44:1231–1237.
29. Pollanen MS, Deck JHN. The mechanism of embolic watershed infarction: experimental studies. *Can J Neurol Sci* 1990;17:395–398.
30. Hupperts RMM, Lodder J, Wilmink J, Boiten J, Heuts-van Raak EPM. Haemodynamic mechanism in small subcortical borderzone infarcts? *Cerebrovasc Dis* 1993;3:231–235.
31. Yonas H, Smith HA, Durham SR, Pentheny SL, Johnson DW. Increased stroke risk predicted by compromised cerebral blood flow reactivity. *J Neurosurg* 1993;79:483–489.
32. Bladin CF, Chambers BR. Clinical features, pathogenesis and computed tomographic characteristics of internal watershed infarction. *Stroke* 1993;24:1925–1932.
33. Vorstrup S. Tomographic cerebral blood flow measurements in patients with ischemic cerebrovascular disease and evaluation of the vasodilatory capacity by the acetazolamide test. *Acta Neurol Scand* 1988;77:3–48.
34. Pedersen EH. Effect of acetazolamide on cerebral blood flow in subacute and chronic cerebrovascular disease. *Stroke* 1987;18:887–891.
35. Powers WJ, Raichle ME. Positron emission tomography and its application to the study of cerebrovascular disease in man. *Stroke* 1985;16:361–376.
36. Lear JL, Ackermann RF, Kameyama M, Kuhl DE. Evaluation of [^{123}I]isopropyliodoamphetamine as a tracer for local cerebral blood flow using direct autoradiographic comparison. *J Cereb Blood Flow Metab* 1982;2:179–185.
37. Kessler RM, Ellis JR Jr, Eden M. Analysis of emission tomographic scan data: limitations imposed by resolution and background. *J Comput Assist Tomogr* 1984;8: 514–522.
38. Kuhl DE, Phelps ME, Kowell AP, Metter EJ, Selin C, Winter J. Effects of stroke on local cerebral metabolism and perfusion: mapping by emission computed tomography of ^{18}FDG and $^{13}NH_3$. *Ann Neurol* 1980;8:47–60.
39. Takano T, Nagatsuka K, Ohnishi Y, et al. Vascular response to carbon dioxide in areas with and without diaschisis in patients with small, deep hemispheric infarction. *Stroke* 1988;19:840–845.
40. van der Zwan A, Hillen B. Review of the variability of the territories of the major cerebral arteries. *Stroke* 1991;22:1078–1084.
41. Fisher CM. Lacunar strokes and infarcts: a review. *Neurology* 1982;32:871–876.
42. Weiller C, Ringelstein EB, Reiche W, Thron A, Buell U. The large striatocapsular infarct: a clinical and pathophysiological entity. *Arch Neurol* 1990;47:1085–1091.